Department of Plant Science, University of Nottingham

TLP6 regulates lateral root angle in *Arabidopsis thaliana*

Joshua Weblin

Supervisor: Dr. Rahul Bhosale, Dr. Adam Binns

Keywords: Root angle, HvEGT1, AtTLP6, gravitropism, *arabidopsis thaliana*

Abstract word count: 257

Report word count: 5399

Research article format report submitted to The University of Nottingham in partial fulfilment of the requirements for the degree of Master of Research in Plant Science.

Abstract

Root architecture plays a critical role in nutrient and water acquisition, as well as providing anchorage. This makes it vital for plant adaptation to environmental changes. A steeper root angle is particularly advantageous for capturing mobile nutrients, accessing deeper water reserves, and improving drought resilience. Previous studies have demonstrated that steeper root angles enhance crop yields under nitrogen and drought stress, underscoring the importance of understanding the mechanisms regulating root angle. In plants, root angle is governed by competing gravitropic and antigravitropic offset (AGO) mechanisms, with gravitropic set-point angles (GSA) dictating root orientation. Recent research in barley and wheat identified EGT1 (Enhanced Gravitropism 1) as a key component of the AGO pathway controlling root angle across all root classes. Moreover, our collaborators have shown that the ortholog in rice also has a conserved function. Despite these findings, little research has explored whether this mechanism is cereal-specific or conserved in non-cereal species such as Arabidopsis *thaliana* (Arabidopsis). To address this gap, we investigated tubby-like proteins (TLPs) in Arabidopsis (AtTLPs), which are implicated in various physiological processes, including root architecture regulation. This study examines the role of AtTLPs in controlling primary root gravitropism and lateral root angle traits. Using in silico protein localization, phylogenomic analyses, and phenotyping of T-DNA mutants of multiple AtTLP family members, we demonstrate that AtTLP6 significantly influences lateral root angle in Arabidopsis, suggesting a conserved role for TLPs in root architecture across species. These findings lay the groundwork for future research aimed at manipulating root angles in diverse crops to enhance stress resilience and nutrient acquisition.

Introduction

The root system plays a critical role in acquiring nutrients and water from the soil, as well as providing anchorage. Consequently, root architectural traits are important to plants' ability to adapt and manage changing environmental conditions. Due to their sessile nature, plants rely on the high sensitivity of roots to perceive physical environmental stimuli and drive changes in growth direction (tropisms) [1]. A steeper root angle is advantageous for capturing mobile nutrients, facilitating easier access to nitrogen and reaching water deeper in the soil. Thus, steeper roots in particular are suggested to be crucial to future crop development. Crop yields under nitrogen stress are substantially better in maize (*Zea mays*) lines with steeper root growth angles [2]. Additionally, change in root angle aids resistance to drought and temperature conditions, as water tends to concentrate in deeper soil layers over time, and so the ability to access this reservoir could increase crop yield if implemented widely [2]. This is particularly important in the coming years due to the increased occurrence of drought and temperature stresses due to climate change [3]. Therefore, a deeper understanding of the mechanisms regulating a plant's gravitropism or antigravitropic pathways that control root angle is crucial. By understanding and manipulating the molecular mechanisms that control root angles, crop varieties can be bred with optimised root angles for enhanced stress resilience or nutrient acquisition.

Root angle in plants is determined by competing gravitropic and antigravitropic offset (AGO) mechanisms. Gravitropic mechanisms include gravity sensing, where the plant recognises gravity vectors through organelles such as statoliths [4]. These sedimentable, starch-filled plastids are directed by gravity and are proposed to interact with the cell membrane as mediators of the signal [5]. This sensing must then be transferred into a signal, to convert the gravity information into a biochemical signal and share this information throughout tissues and organs through molecules such as the phytohormone auxin. This can lead to asymmetric organ growth, differential cell division, and elongation and the termination of the signal once the desired angle has been achieved [6]. The angles of different sets of roots are often different to limit competition between the roots of the same plant. These distinct angles are known as GSA. GSA can be defined as an angle that is maintained with respect to gravity regardless of the parental organ which they develop from [7]. In Arabidopsis, the gravitropic mechanism has been observed within the tip of the root, leading to a formation of a lateral auxin gradient causing unequal growth of epidermal cells within the elongation zone causing

bending [8]. AGO mechanisms are a relatively new domain of research but have been suggested to be dependent on auxin transport where GSAs are maintained by the two opposing auxin fluxes [9].

Root systems in Arabidopsis differ significantly from those in many crop species. Arabidopsis primarily features a simpler root architecture, composed of a primary root and fewer lateral roots, which contrasts with the more complex root systems seen in crops. Although crops form primary and lateral roots in a manner roughly similar to Arabidopsis, there are some key differences [10]. For instance, crops often possess various root classes, such as seminal, adventitious, and fibrous roots, allowing them to adapt effectively to different soil conditions and optimize nutrient and water uptake [11]. These additional root classes utilise different GSA setpoints to enhance the plant's ability to explore the soil and utilize resources efficiently without self-competition [12], making them essential for agricultural productivity.

Previous studies on *HvEGT1* (*ENHANCED GRAVISTROPISM 1*), a gene encoding a TLP in barley (*Hordeum vulgare*), has shown that mutating it leads to a strikingly steeper root angle phenotype in all root classes. HvEGT1 appears to function as a component of an anti-gravitropic offset mechanism [8]. The proposed mechanism involves regulating cell wall stiffness in elongating root cortical tissue, counteracting the gravitropic machinery [8]. As a protein from this family has been shown to control root architecture in barley and wheat, this suggests a conserved function within other cereal crops, including rice, as recently observed by our collaborators. However, no research has yet explored whether this mechanism is cereal specific or conserved in non-cereal species such as Arabidopsis. This conservation of protein structure, combined with previous studies in Arabidopsis showing links between AtTLPs and hormone pathways that regulate various aspects of plant growth and development such as ABA and osmotic stress pathways [13], make the AtTLP protein family a promising candidate for further gene function characterisation. The *AtTLP* gene family also exhibits overlapped but distinct expression patterns in various tissues, including the roots [13]. Demonstrating a conserved function in Arabidopsis could offer deeper insights into these mechanisms. Additionally, the discovery of a non-cereal homolog would indicate a broader evolutionary role for this gene family in root angle control. This would also have significant implications for manipulating root angles in a wider range of crops beyond cereals. Arabidopsis is a much easier model system for analysing molecular mechanisms compared to cereals such as barley, due to its small genome, rapid germination, short life cycle, and ease of cultivation. Additionally, well established protocols and genetic tools [14], e.g. T-DNA from The Nottingham Arabidopsis Stock Centre (NASC) repositories, make Arabidopsis an ideal choice for such studies.

Further evidence for an AtTLP impact and possible function within root angle regulation are the interactions between Arabidopsis Skp1-like proteins (ASK) due to the conserved F-box region within AtTLPs. These are key components of Skp1-Cullin-F-box (SCF) E3 ubiquitin ligase complexes [15]. These complexes play critical regulatory roles in many biological processes by targeting specific proteins for degradation via the ubiquitin-proteasome pathway [15]. The F-box component of the protein complex confers substrate specificity, determining which proteins will be ubiquitinated and subsequently degraded.

In this MRes project, I conducted systematic in silico protein localization, protein structure, and phylogenomic analyses to identify F-box and TLPs in Arabidopsis. Additionally, I performed genotyping, genetic crossing and phenotyping experiments to identify a key mutant with defects in gravitropic responses and lateral root Gravitropic Set-Point Angles (GSA). We show that At*TLP6* is a potential *HvEGT1* ortholog that controls lateral root angle phenotype in Arabidopsis. This may suggest that function of such proteins in regulating root angle is not specific to cereals.

Materials and Methods

Plant materials and growth conditions.

Seeds of T-DNA insertion mutant lines for various TLPs (Table 1) were obtained from NASC. Columbia-0 (Col-0) and Columbia-03 (Col-3) ecotypes were used as wildtype for root gravitropic and

lateral root angle phenotyping assays. To investigate functional redundancy, *Attlp2* and *Attlp3* single mutants were crossed to generate a double mutant. All seeds were surface sterilized using chlorine gas and plated on ½ MS medium (pH 5.8; 0.1 mM NaOH was used to adjust pH) containing 1% agar. Plates stratified at 4°C for 48 hours and then transferred to a growth chamber set at 21°C under a 16-hour light/8-hour dark cycle.

TLP		Allele	Background	SALK line	Forward Primer Sequence (FP)	Reverse Primer Sequence (RP)	Wild Type Product size (BP)	Mutant Product size (BP)
TLP1	*AT1G76900*	*tlp1-1*	Col-0	SAIL_905_D01	ACGGAGAAGACGAGGAAAAAC	GGAAATGTGATTTTGCCTGAG	1119	~650
		tlp1-2	Col-0	SALK_093037C	TCGACCAAAGCCAAATGATAG	GACACTCCACACATCAAATGC	1088	~500
TLP2	*AT2G18280*	*tlp2-1*	Col-0	SALK_103619C	GGATAGGTCTGGTTTTCTGGG	ATGATTGCCTTTGCATGACTC	1091	~720
		tlp2-2	Col-0	SALK_058100C	CCTTGTGATTGCGAATTTTTC	AAGATCGGAAAGAGAAAACGC	1237	~750
TLP3	*AT2G47900*	*tlp3-1*	Col-0	SALK_072994	GGAACCCAAGACGTTAAGCTC	TCGTTGAGATCTCGTTCGTTC	1131	
		tlp3-2	Col-0	SALK_131745	ATTTAGACTTCAATTCGGCCC	CCCTAATAAACCCACATTCGG	1169	~680
TLP5	*AT1G43640*	*tlp5-1*	Col-0	SALK_069659C	TTTTGGTGAAAAATGGTATACATC	CTCAGAAACGACATTTTTCCG	1245	~730
		tlp5-2	Col-0	SALK_030876C	CCCACTTTCAACAAGTATGGC	TTGTTTTGCTACCCACTCAAAG	1191	
TLP6	*AT1G47270*	*tlp6-1*	Col-0	SAIL_618_F07	TGTGAATTCAACTTTTTGGGG	AACAAAAGCGACAAATCCATG	1180	~690
		tlp6-2	Col-0	SALK_019494	CAATGTGTGACCTCCCTCTTC	GGCTTCTACCTTCTCCTTTGG	1213	
TLP7	*AT1G53320*	*tlp7-1*	Col-0	SALK_092324C	TGAAAATGATCCTTTTGCCAG	CGCTTGCGTTTCTAAGAAATG	1025	
TLP9	*AT3G06380*	*tlp9-1*	Col-3	SAIL_130_E12	CGTTGTTAACATGTCCGATCC	AAGTGGTGTTGGTGAGAGACG	1002	~600
		tlp9-2	Col-0	SALK_016678C	AACAAACCTTCCCTCTTCCTG	CAAAGAGAAGCAACGCGTATC	1095	~520
TLP10	*AT1G25280*	*tlp10-1*	Col-3	SAIL_293_H09	AAGACTCCAAGTTCAACGGTG	GAAGAGATATGCAAGGCATCG	1116	~650
		tlp10-2	Col-0	SALK_028746C	AAGCATTTTTGTGAGAGTCCC	AACTCCTCCTTGACAAGCTCC	1166	
TLP11	*AT5G18680*	*tlp11-1*	Col-0	SALK_085537C	AAAAGGGACCTTTCCACACAC	CATCTCTCTCAAGCAGGTTCG	1238	
		tlp11-2	Col-0	SALK_070225C	TAGCGTCGGTTGAAACAAAAG	AGGCTGCAGAAGATACACACC	1065	~580

Table 1. Mutant lines for *AtTLPs,* identified as relevant for testing conserved function with HvEGT1, were obtained from NASC due to similar familial structure [16], with SAIL and SALK lines initially sourced from [17] and [18] respectively. Background represents the wild-type genetic background for each allele. Product size indicates the length of the PCR product expected from a positive result for the wild-type allele using FP+RP. Mutant product size refers to the expected size of the band from the T-DNA insert PCR product using BP with the correct directional border primer.

Mutant genotyping

T-DNA mutants were sourced from NASC, with selected alleles positioned near the start codon or within the N-terminal coding region of the *AtTLP* genes [16] to maximize the chance of obtaining functional knockouts (Figure 1). DNA was extracted from young leaves using Edwards buffer [19] [containing 200mM Tris-HCl pH 8.0, 250mM NaCl, 25mM EDTA, 0.5% SDS], and genotyping was performed via PCR. Each PCR reaction included 1 µL of template DNA, 10 µL of VWR Red Taq DNA Polymerase Master Mix [made up of Tris-HCl pH 8.5, (NH4)2S04, 3.0 or 4.0 mM MgCl2*, 0.2 % TweenÒ 20, 0.4 mM of each dNTP, 0.2 units/µl VWR Taq polymerase Inert red dye and a stabilizer], 0.4 µL of 10 µM SALK or SAIL primers, and distilled water to a total volume of 20 µL. To test for the T-DNA insert being homozygous, primers matching forward and reverse for each side of the TDNA allele were included in one reaction and a primer matching either the SALK (LBb1.3) or SAIL (LB2) T-DNA insert and the reverse primer (matching product lengths mentioned in table 1). Gradient PCR with annealing temperatures from 50°C to 70°C was used to identify optimal temperature conditions, with 58°C found to be effective. The optimised PCR protocol included, an initial denaturation of 95°C for 2 minutes, then 35 repeats of denaturing at 95°C for 30 seconds, annealing at 58°C for 30 seconds and extension at 72°C for 1 minute. After the repeats, a final extension at 72°C was held for 5 minutes. Following PCR, homozygous mutants were confirmed, bulked to obtain seeds; while growing in the growth room, individual plants were bagged separately to prevent cross-contamination. Seeds were then harvested from mature plants for further experimentation.

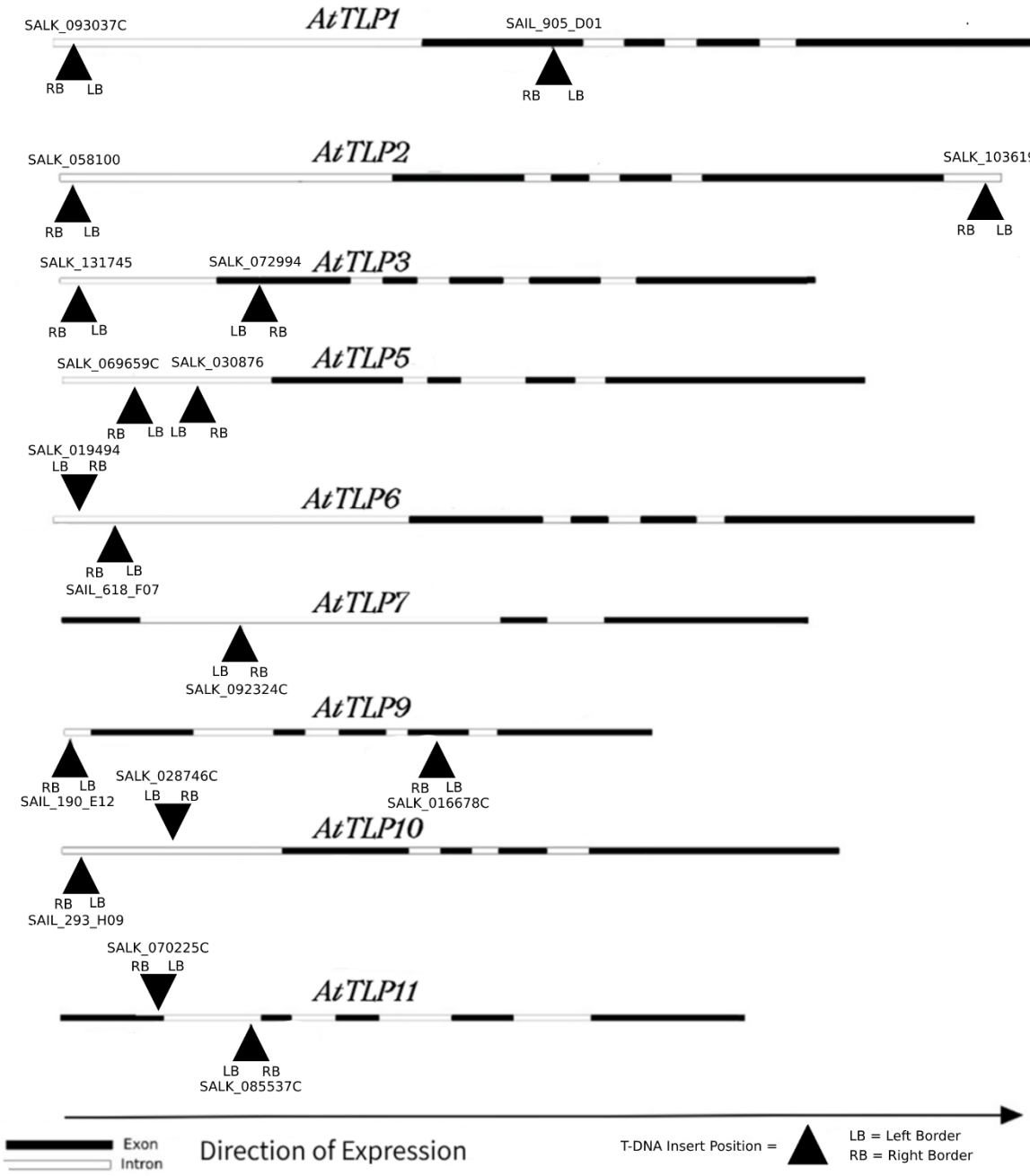

Figure 1. Structure of *AtTLPs* and location of T-DNA inserts [17] [18]. Black bars represent the Exon, with black lines representing the introns. White bars before the start of the first intron are inserts within the upstream sequence. The black triangles indicate the location of the insertion point within the gene with left (LB) and right (RB) border primers marked.

In Silico Protein Localisation, Structure, and Phylogenetic Analysis

The potential functions of the *AtTLP* family in Arabidopsis were analysed using structural and phylogenetic tools. Structural comparison of AtTLP proteins with barley HvEGT1 was performed using the DALI server, which identified several high-confidence structural homologs (Table 2). DALI allows us to submit a query protein, in this case HvEGT1, and compare its structure to other proteins. This was performed with the AlphaFold database for HvEGT1 against the AtTLP family to identify not only sequence similarity and conserved domains, but the folding structure as well [20].

The predicted subcellular localization of each AtTLP was determined using the Plant-mSubP prediction mode, which is a computational framework developed for the prediction of protein

subcellular localization in plant proteomes. It employs an integrated machine-learning approaches to achieve this prediction.

Additionally, phylogenetic analysis was conducted using the neighbour-joining method with 500 bootstrap replicates in MEGA 11, utilising the Poisson model on amino acid sequences and established phylogenomic pipelines [21] to understand the relationships between AtTLP proteins and HvEGT1, as well as their potential functional redundancies. Sequence folding predictions and structural similarities were analysed based on the pipeline outlined in the paper.

Root Gravitropism and Lateral Root Angle Phenotyping

Root phenotyping was performed on homozygous mutants using both gravitropic and lateral root angle assays. For primary root bending analysis, 20 seeds per genotype were grown vertically on ½ MS plates for 10 days before being subjected to 90° reorientation within an infrared imaging robot. Images were captured hourly for 12 hours, and root angles were quantified using ImageJ. Measurements were taken at 0-, 6-, and 10-hours post-reorientation, with root length also measured from the hypocotyl to the tip. For lateral root angle analysis, plants were grown for 14 days and imaged using RootNav, which was used to map root architecture and measure the width profile. Each experiment was performed in triplicate for statistical significance.

Measurements and statistical analysis

All results were checked for normal distribution using the Shapiro-Wilk test, if they were distributed normally then they were analysed using Welch's T-test, else they were performed using a Mann-Whitney U-test. For all values the p value threshold was <0.05.

Results

Mutant Genotyping

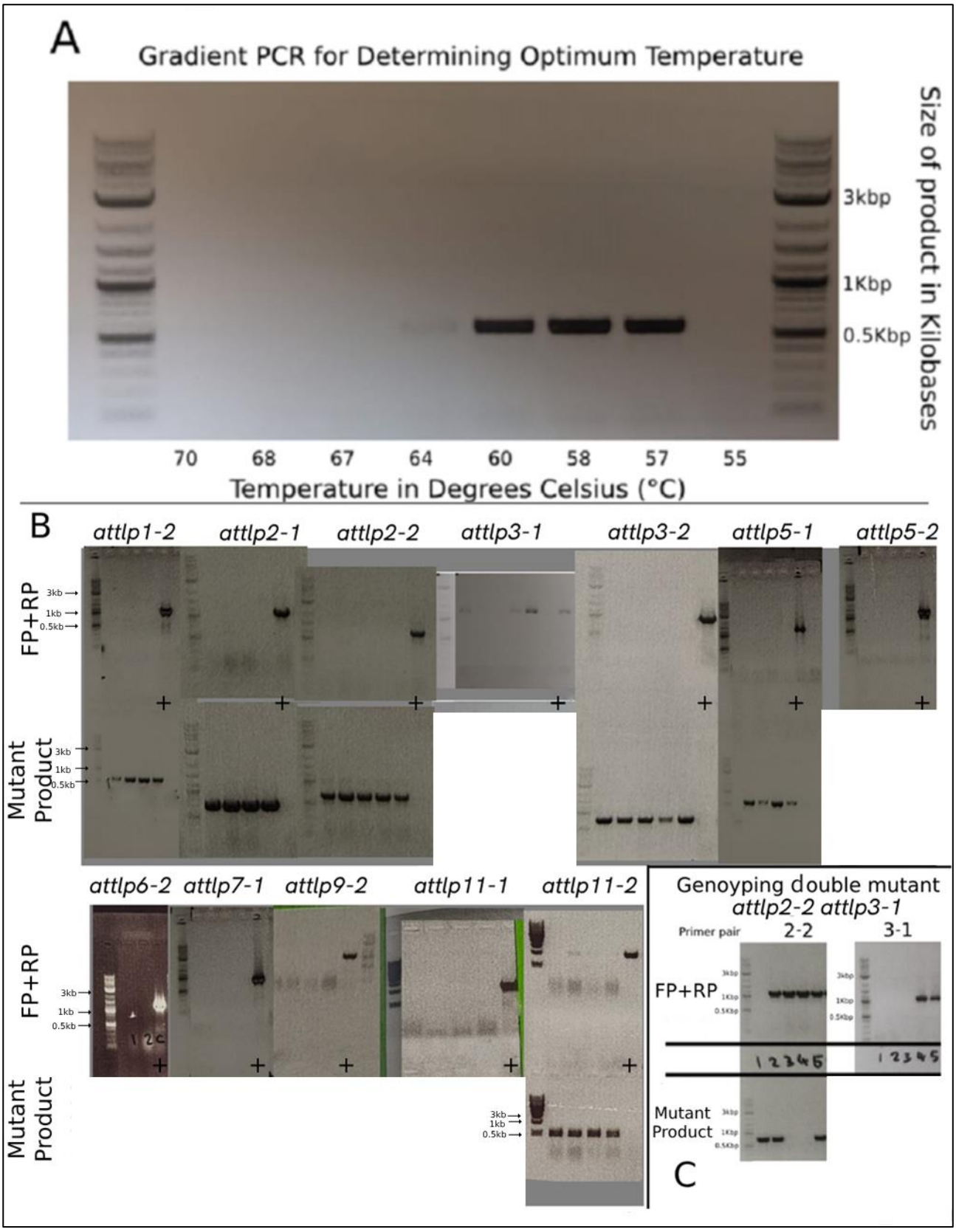

Figure 2. A. An example of the type of gradient PCR using primers FP (Forward primer) +RP (Reverse primer) for attlp3-1 to determine optimum annealing temperatures. The range was 55°C to 70°C B. Single mutant genotyping of attlp mutants was done using FP and RP primer combinations where a band indicates the presence of wild-type DNA. Further validation was done using tDNA border primer (LB) with gene specific reverse primer (RP). Black (+) indicates the wild-type Col-0 control used as a positive control. C. PCR results for the double mutant attlp2-2 and attlp3-1. Ladder used in all PCR genotyping

was 1 kb Plus DNA Ladder with positions of the 0.5, 1, and 3Kb bands marked. A negative control was present for all but is not displayed.

We repeated the annealing temperature gradient analysis (*figure* 2A) for all primer pairs and found that 58°C was the optimum. This gave us a strong band at the correct length as predicted by Table 1 of 1131 for wild type *attlp3-1*. Figure 2B displays all the T-DNA inserts for which a homozygous mutant was obtained. Genotypes for which a homozygous mutant was not able to be obtained include *attlp1-1*, *attlp6-1, attlp7-2*, *attlp9-1*, *attlp10-1*, and *attlp10-2*. Unfortunately, no further study on any *attlp10* mutants was possible as neither allele was able to be successfully genotyped as homozygous for the T-DNA insert. Due to issues with the T-DNA insertion direction and protocol we are unable to validate the insertion of the T-DNA insert in *attlp3-1, attlp5-2, attlp6-2, attlp7-1, attlp9-2,* and *attlp11-1.* For all but attlp3-1 the lines obtained from NASC were isolated homozygous lines and as such the lack of a band within the control for the wild type confirms the T-DNA insert.

All samples genotyped (*figure 2C*) for *attlp2-2* are homozygous for the T-DNA mutant allele with no bands in the wild type. Both results showed for *attlp2-2* and wild type control saw correct lengths of 603-903 and 1091 respectively. Two Likely double homozygous mutants were also observed for *tlp3-1*(*figure 2C*), with samples 2 and 3 both not showing a band within the wild type. This however cannot be a sure confirmation of the T-DNA for the *attlp3-1* insertion.

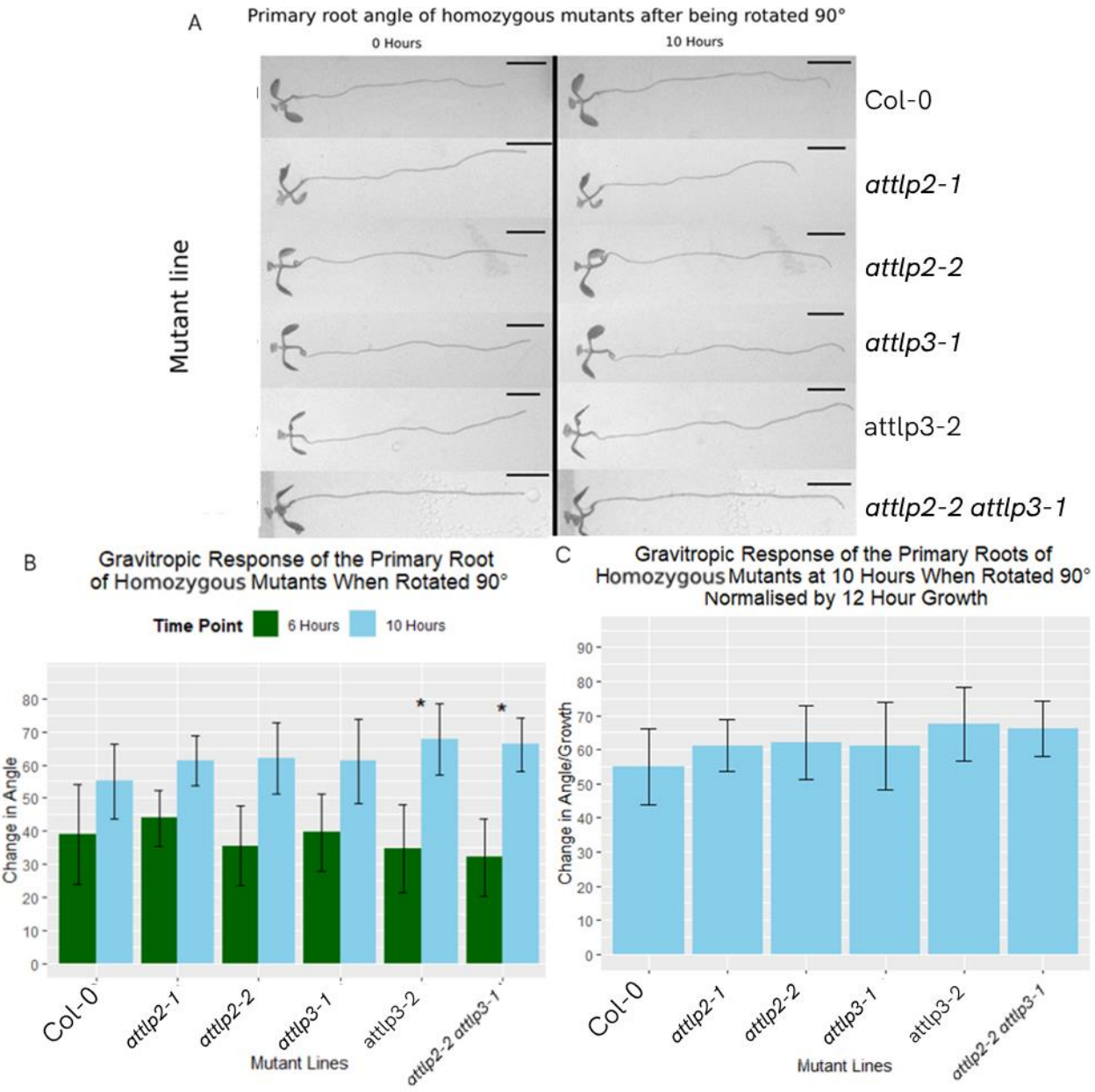

Figure 3. A. Infrared images of 10-day old plants used for the phenotyping of T-DNA inserts for *attlp2*, *attlp3*, and *attlp2-2 attlp3-1* at 0 and 10 hours after being rotated 90°. Black bars represent 5mm. B. The mean change in angle from 0 hours to 6 hours, then 10 hours. Asterisks represent significant differences where $p<0.05$ between the *attlp* mutants and Col-0, with Col-0 having a population of 14. The p-values for each significant mutant from a Welch's T test as well as N being their population displayed as such. *attlp3-2* p=0.003418 n=18, *attlp2-2 attlp3-1* p=0.004758 n=19. Asterisks indicate significant difference where $p<0.05$. C. The mean change in angle from 0 hours to 10 hours when normalised for 12 hours of growth. No significant difference in angle by growth when compared with a Welch's T-test.

Phenotyping of Homozygous Mutant Lateral Roots

A

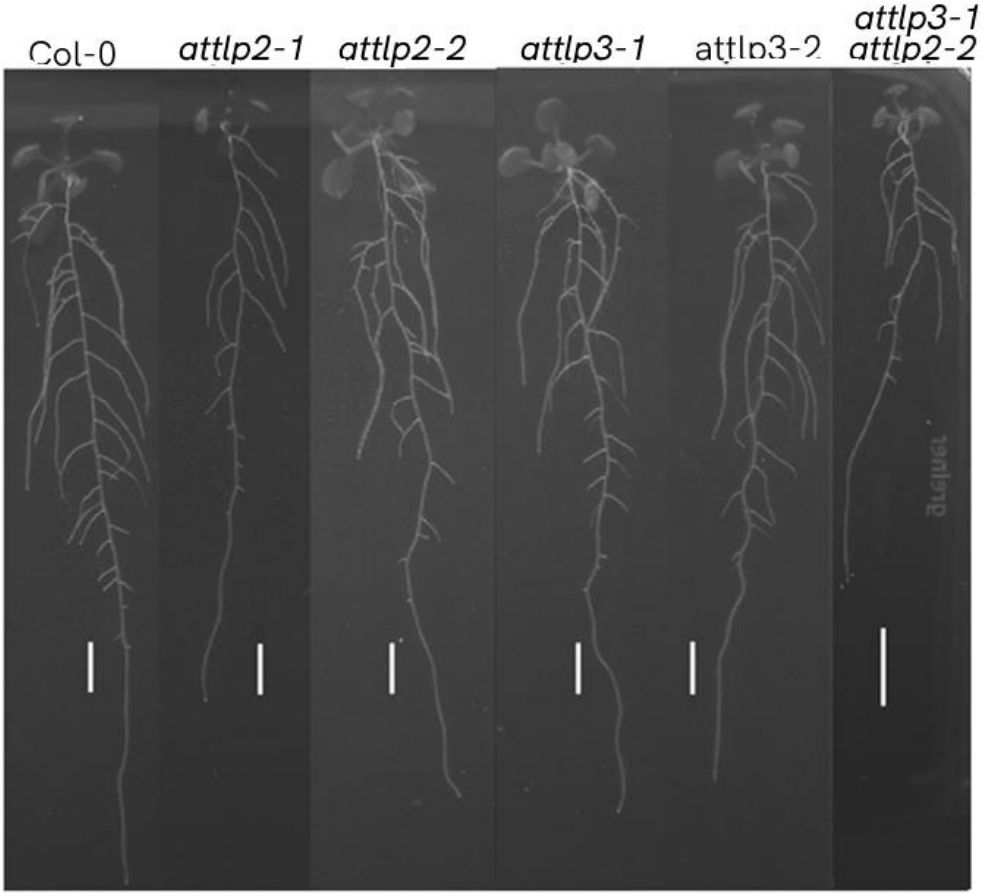

B

Width profile of lateral root development for homozygous mutants

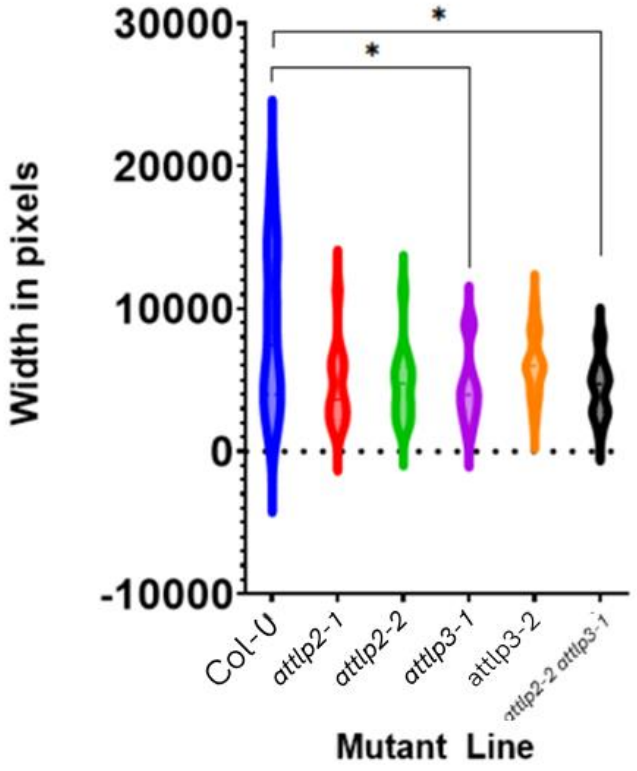

Figure 4. A. Images of 12-day old plants used for the phenotyping of lateral root structure for T-DNA inserts for *attlp2*, *attlp3*, and *attlp2-2 attlp3-1*. Significant changes in root phenotypes were shown for *attlp3-1* and *attlp2-2 attlp3-1* when compared with Col-0. White bars represent 5mm. B. The mean width in pixels for each individual mutant plotted onto a violin plot. Asterisks represent significant differences ($p<0.05$) between the *attlp* mutants and Col-0 with a population of 14, with p-values for each significant mutant from a Welch's T test as well as N being their population displayed as such. *attlp3-1* p=0.0243 n=15, *attlp2-2 attlp3-1* p=0.0187 n=17.

Previously suggested orthologs of *HvEGT1*, *AtTLP2* and *AtTLP3*, do not show primary root gravitropism or lateral root angle phenotypes

Based on transcriptomics and GO enrichment analysis studies conducted by Fusi et al. (2022) [8], *AtTLP2* and *AtTLP3* were suggested as potential orthologs of *HvEGT1* due to their association with ROS and cell wall processes, which have been implicated in HvEGT1-mediated root growth angle regulation. To validate this hypothesis and investigate their role in root gravitropism and lateral root development, we obtained the homozygous mutants *attlp2* and *attlp3 (figure 2)* and conducted phenotyping assays. Our results demonstrated that while *attlp3-1* shows increased bending when compared with the wild-type control (Col-0) (*figure 3B)*, neither *attlp2* nor *attlp3* mutants showed enhanced primary root gravitropic bending compared to the wild-type control (Col-0) when normalised by growth rate over 12 hours (*figure 3C*). Furthermore, we generated *an attlp2-2 attlp3-1* double mutant to explore any potential synergistic or genetic redundancy effects. However, even in the double mutant, we did not observe any significant differences in root gravitropic bending response when normalised by growth rate. Conversely, our lateral root angle measurements showed a significant difference in *attlp3-2* and *attlp2-2 attlp3-1* (*figure 4B*). These findings suggest that AtTLP2 and AtTLP3, while potentially related to HvEGT1 based on their functional associations, do not play a distinct direct role in regulating root gravitropism, with only partial impact on lateral root angle phenotype in Arabidopsis.

Possible ortholog of HvEGT1 found in AtTLP6 from In Silico Protein Localisation, Structure, and Phylogenetic Analysis.

To continue our attempt to find an AtTLP homolog of HvEGT1 we investigated the entire AtTLP family within Arabidopsis, finding 11 within its genome. AtTLPs can be identified by their structure; the signature tubby domain comprises of a closed β barrel consisting of 12 anti-parallel strands, surrounding a central hydrophobic α helix [22]. Experiments on this domain suggest that the tubby domain interacts with certain membrane phosphoinositide's, predominantly phosphatidylinositol 4,5-bisphosphate (PIP_2) [22]. TLPs are widely conserved across eukaryotic organisms, including the plant kingdom and share a typical carboxyl (C) -terminal Tubby domain for their proper tethering to the plasma membrane by binding specific phosphatidylinositol 4,5-bisphosphates [13]. While the C-terminal Tubby domain of TLPs is highly conserved, within plants the (N) – terminal domain features a conserved F-box domain [13]. The F-box domains allow them to participate in the SCF (Skp1-cullin-f-box) E3 ubiquitin ligase complex, which in turn allows for their substrate proteins to be targeted for ubiquitination and degradation, although TLP substrates have yet to be formally identified [13].

To explore the potential functions of the TLP family within Arabidopsis, we utilized the DALI server for structural comparison with HvEGT1 [23]. DALI identified several high-confidence structural homologs as seen in Table 2. From this we can distinguish that AtTLP2, AtTLP3, AtTLP6, AtTLP9, and AtTLP11 all share significant structural similarities due to their high Z-score, which overcome the cutoff of n/10 -4[23], where n is the number of residues in the structure [20]. These alignments highlight regions of structural conservation. The process also shows that the 3D visualization of the superimposed structures for AtTLP2, AtTLP3, AtTLP6, AtTLP9, and AtTLP11 have significant overlap with that of HvEGT1.

PDB Description	AGI	Z	rmsd	lali	nres	%id	Z score cutoff	overcome Z score?
TUBBY-LIKE F-BOX PROTEIN 1	AT1G76900	38.5	4	382	455	54	41.5	FALSE
TUBBY-LIKE F-BOX PROTEIN 2	AT2G18280	39.2	9.2	373	394	60	35.4	TRUE
TUBBY-LIKE F-BOX PROTEIN 3	AT2G47900	41.4	5.4	392	406	54	36.6	TRUE
PUTATIVE TUBBY-LIKE PROTEIN 4	AT1G61940	6.6	4.3	117	265	42	22.5	FALSE
TUBBY-LIKE F-BOX PROTEIN 5	AT1G43640	37.6	3.9	374	429	48	38.9	FALSE
TUBBY-LIKE F-BOX PROTEIN 6	AT1G47270	39.9	11.6	366	413	57	37.3	TRUE
TUBBY-LIKE F-BOX PROTEIN 7	AT1G53320	32.5	8.4	323	379	52	33.9	FALSE
TUBBY-LIKE PROTEIN 8	AT1G16070	23.6	19.8	263	397	25	35.7	FALSE
TUBBY-LIKE F-BOX PROTEIN 9	AT3G06380	37.1	7.2	337	380	52	34	TRUE
TUBBY-LIKE F-BOX PROTEIN 10	AT1G25280	39.7	5	395	445	52	40.5	FALSE
TUBBY-LIKE F-BOX PROTEIN 11	AT5G18680	39.1	8.8	354	389	51	34.9	TRUE

Table 2 All 11 AtTLPs compared structurally to HvEGT1 showing if they are significantly similar. AtTLPs that have a Z score above the cutoff are significantly similar. Cutoff is designated at n/10-4 where n is the number of residues [23]. RMSD: Root-mean-square-deviation shows the average distance between the atoms of superimposed molecules. Lali: The number of residues aligned. nres: Total number of residues. %id: The percent identity. 'Strong matches' have a sequence identity of above 20% [20].

To further study the relationships between the significant proteins and HvEGT1 we performed multiple analysis for phylogeny including sequence matching and folding predictions based on the pipeline outlined in this paper [21]. It was found that AtTLP2 and AtTLP6 formed a clade with HvEGT1, and other similar proteins found in different species as shown in figure 5C. We also discovered that AtTLP4 and AtTLP8 were not worth the continued study in this regard. Previous studies have suggested that AtTLP4 may be a pseudogene [13, 24] which may explain this. Furthermore, AtTLP8 was removed from further testing as it does not contain a conserved F-box domain [24] and thus lacks a key structure found in HvEGT1. As seen in figure 5A, AtTLP4 and AtTLP8 clearly fold in a manner unlike HvEGT1 and so the stark lack of a similar structure indicates no likely relationship to HvEGT1. Using phylogeny and identifying conserved residues, such as the PIP2 binding site, may in the future, allow us to predict more accurately which of the AtTLPs, if any, may conserve function [25].

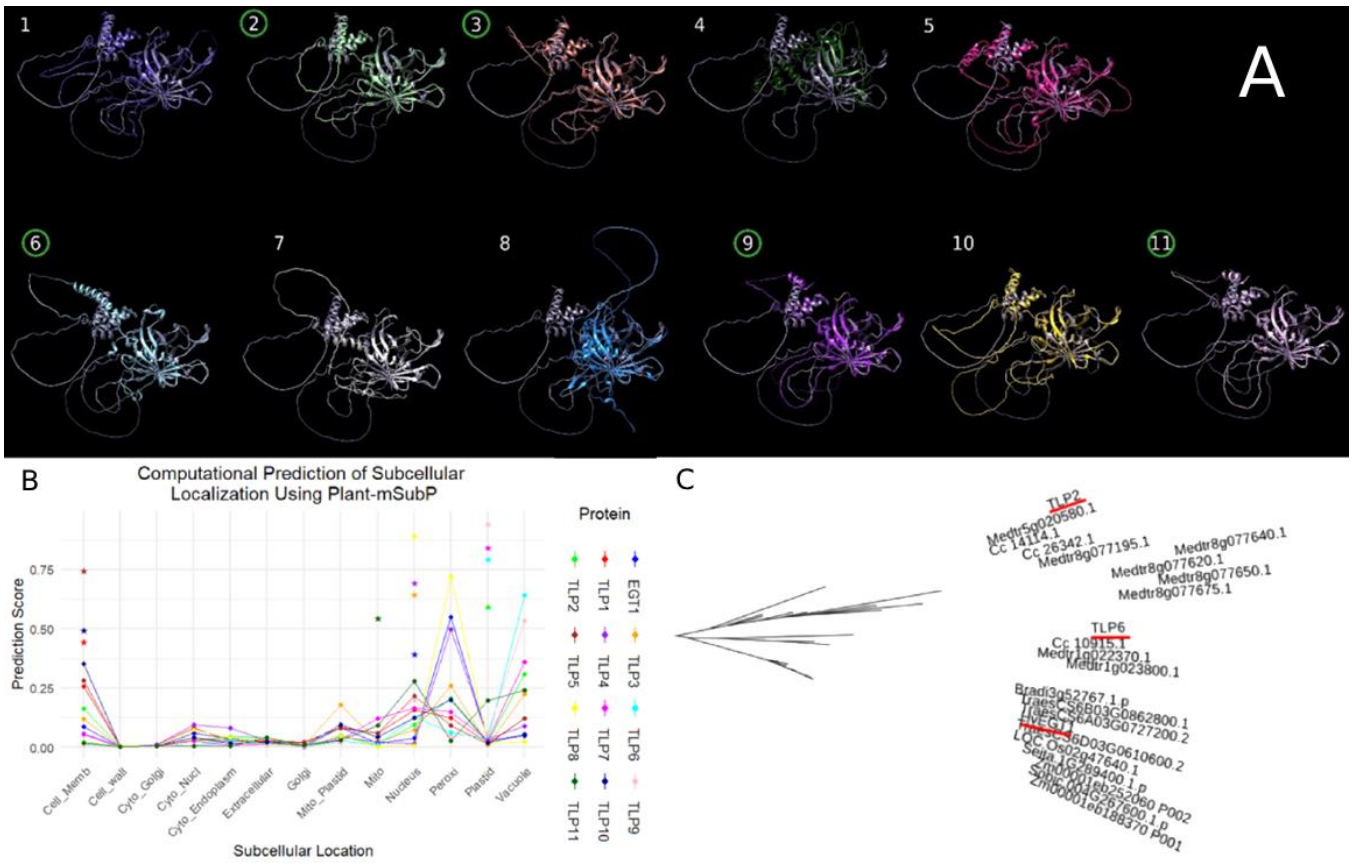

Figure 5 A. Overlapped aligned 3D protein structure with the top left number equalling the AtTLP it represents (1 = AtTLP1) superimposed over the white HvEGT1 protein. The green rings around the numbers represent the significantly similar proteins as shown in table 1. B. The predicted subcellular localisation of each AtTLP with a coloured asterisk matching the overall predicted localisation based on the Plant-mSubP predication model [26]. The coloured lines show the relative prediction score for likelihood for the protein to localise at the relevant location. Cell_memb = Cell membrane, Cell_wall = Cell wall, Cyto_golgi = cytoplasmic Golgi Apparatus, Cyto_nucl = Cytoplasmic nucleus, Mito_plastid = Mitochondrial plastid, Mito = Mitochondrial, Peroxi = Peroxisomes. C. Resulting clade of proteins most similar to HvEGT1 after analysis though the method outlined previously [21]. HvEGT1, AtTLP2, and AtTLP6 are underlined in red.

From figure 5C we can see that AtTLP6 has the closest sequence to HvEGT1 when compared by structure, sequence, and folding patterns. These results allow us to predict that it is more likely to have a similar function to HvEGT1 than AtTLP2 and AtTLP3. The fact that it localises in a similar pattern, if not having the same predicted localisation as seen in figure 5B, further suggests that it may have similar functions within the cell. However, all inferences based off of protein structure are made from in silico analysis following trends and likelihoods, where further study performing these comparisons in vitro or vivo.

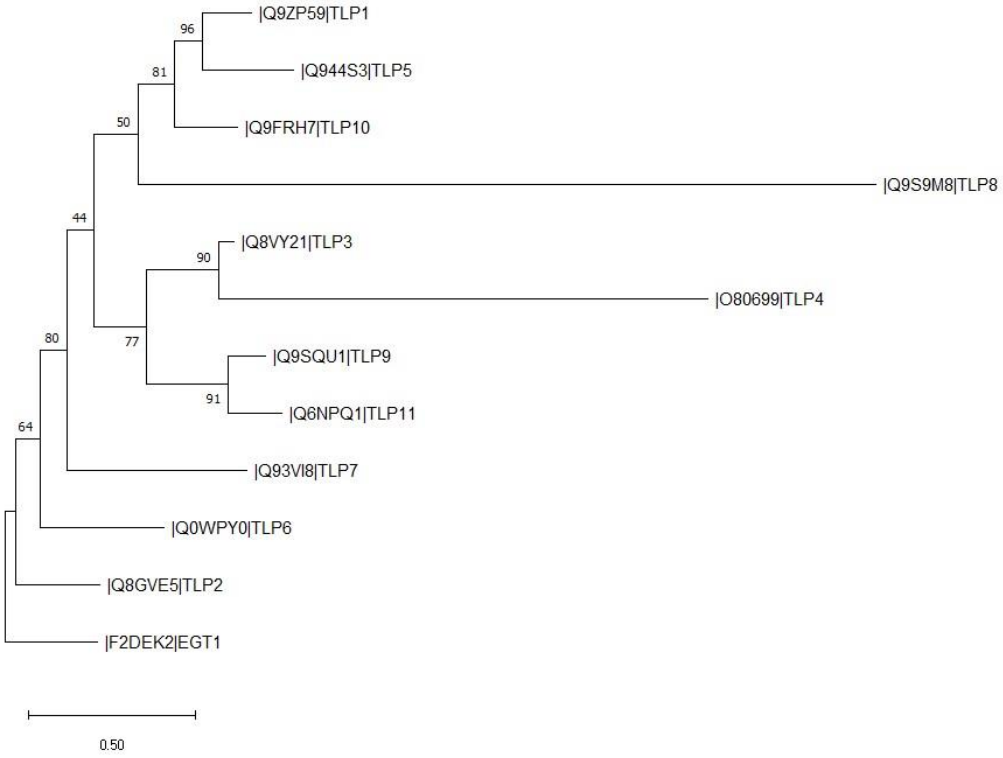

Figure 6. A phylogenetic tree displaying the *e*volutionary history of the AtTLPs, with HvEGT1 as the root, was inferred using the Neighbour-Joining method [27]. The optimal tree is shown. The percentage of replicate trees in which the associated taxa clustered together in the bootstrap test (500 replicates) are shown next to the branches [28]. The evolutionary distances were computed using the Poisson correction method [29] and are in the units of the number of amino acid substitutions per site. This analysis involved 12 amino acid sequences. All ambiguous positions were removed for each sequence pair (pairwise deletion option). There were total of 500 positions in the final dataset. Evolutionary analyses were conducted in MEGA11 [30].

Figure 6 indicates a fairly conserved relationship between the AtTLPs in regard to their C termini and F-box, indicating the possibility of redundant pathways within the gene family, especially across AtTLP9 and AtTLP11 due to their high similarity and relative closeness to HvEGT1 when compared with other clades. We can confirm this against results from other papers which indicate up to 80% amino acid similarity within these regions [24]. These results confirmed our decision to include all AtTLPs apart from AtTLP4 and AtTLP8 in our testing, as while they may not be significantly similar to HvEGT1, they maintained the same general structure. The branch length here indicates that AtTLP4 and AtTLP8 have undergone a significant amount of evolutionary divergence from other members within their respective clades and therefore have been exposed to genetic drift and have not had a strong selection pressure for their protein coding sequences to be conserved. Furthermore, other studies into AtTLPs also concluded that AtTLP4 and AtTLP8 could be excluded from analysis of the protein family [24]. These findings are important for this study to not include any selection bias and observe all the possible phenotypes. This suggests that while AtTLP2 and AtTLP6 are the most likely to be an ortholog within Arabidopsis due to the closeness to HvEGT1, which matches what was predicted in figure 5C, there may be some phenotypes shown in other clades.

Mutant *attlp6-2* shows differences in primary root gravitropism and lateral root angle phenotype

Based on the observations made during our in-silico research, we endeavoured to investigate the role of AtTLP6 as a potential ortholog of HvEGT1 in Arabidopsis. To test this, we attempted to analyse the bending response of *attlp1, attlp5, attlp6, attlp7, attlp9, attlp10,* and *attlp11*. Seed from the

identified double homozygous mutants was collected and were subjected to a phenotype analysis (*figure 7*).

Our initial measurements of root bending angle revealed significant differences in *tlp3-2*, *tlp9-2*, and *tlp11-2* mutants (*figure 7B*). However, to account for potential variations in root growth rate, this data was normalized by the primary root growth over 12 hours (*figure 7C*). Notably, *attlp6-2* did not show a significant change in root bending angle, which was likely due to its significantly shorter overall root growth, limiting its ability to exhibit a pronounced response to gravitropic stimuli. When this was normalised to growth rate, we found that *attlp6-2* and *attlp11-2* showed significantly faster root gravitropic bending response when compared to Col-0. Our lateral root angle measurements *(figure 8A)* further showed a significant difference between Col-0 and *attlp6-2*, with at*tlp6-2* showing a narrower lateral root profile than Col-0(*figure 8B*). However, the same relationship was not shown for *attlp11-2*. These findings suggest that AtTLP6 could play a distinct role in regulating both root gravitropism and lateral root angle and suggests that AtTLP6 could be described as a functional homolog of HvEGT1.

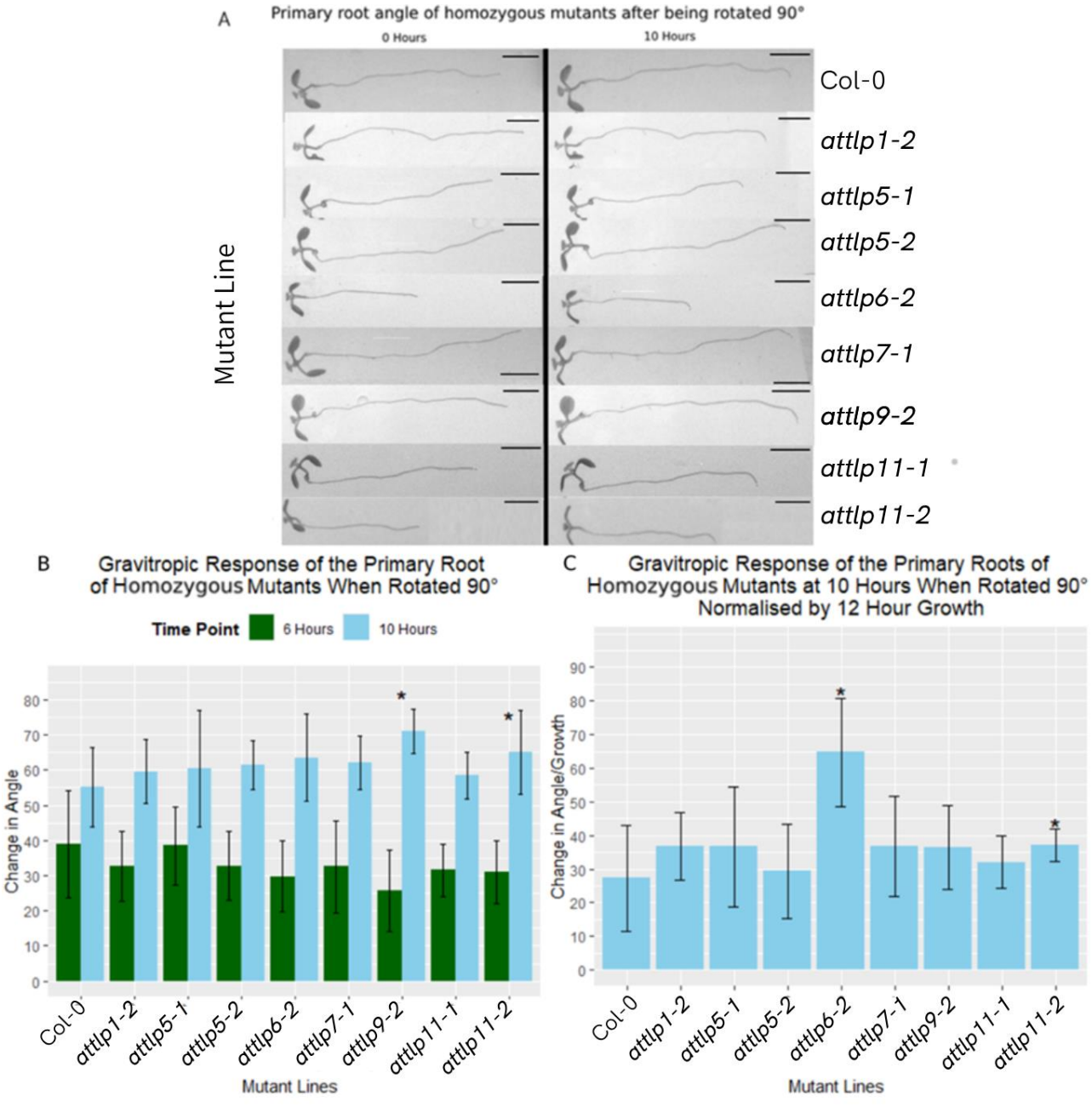

Figure 7 A. Infrared images of primary roots of 10-day old plants used for the phenotyping of genotyped T-DNA inserts for *attlps1,5,6,7,8,* and *11* at 0 and 10 hours after being rotated 90°. Mutants *attlp6-2* and at*tlp11-2* both showed significant changes in response to being rotated when compared to Col-0, with faster bending relative to growth. Black bars represent 5mm. B. The mean change in angle from 0 hours to 6 hours, then 10 hours. The asterisks represent significant differences between the *attlp* mutants and Col-0 (n=14). p-values for each significant mutant from a Welch's T test as well as n being their population displayed as such, *attlp9-2* p=0.0001459 n=14, and *attlp11-2* p=0.02741 n=12. C. The mean change in angle from 0 hours to 10 hours when normalised for 12 hours of growth. T-DNA mutants *attlp6-2* p= 0.00152 n = 8 when compared to Col-0 using Mann-Whitney U test as results were not normally distributed and *attlp11-2* p=0.04327 n=12 both showed a significant difference in angle by growth when compared with Col-0 (n=14) by a Welch's T-test.

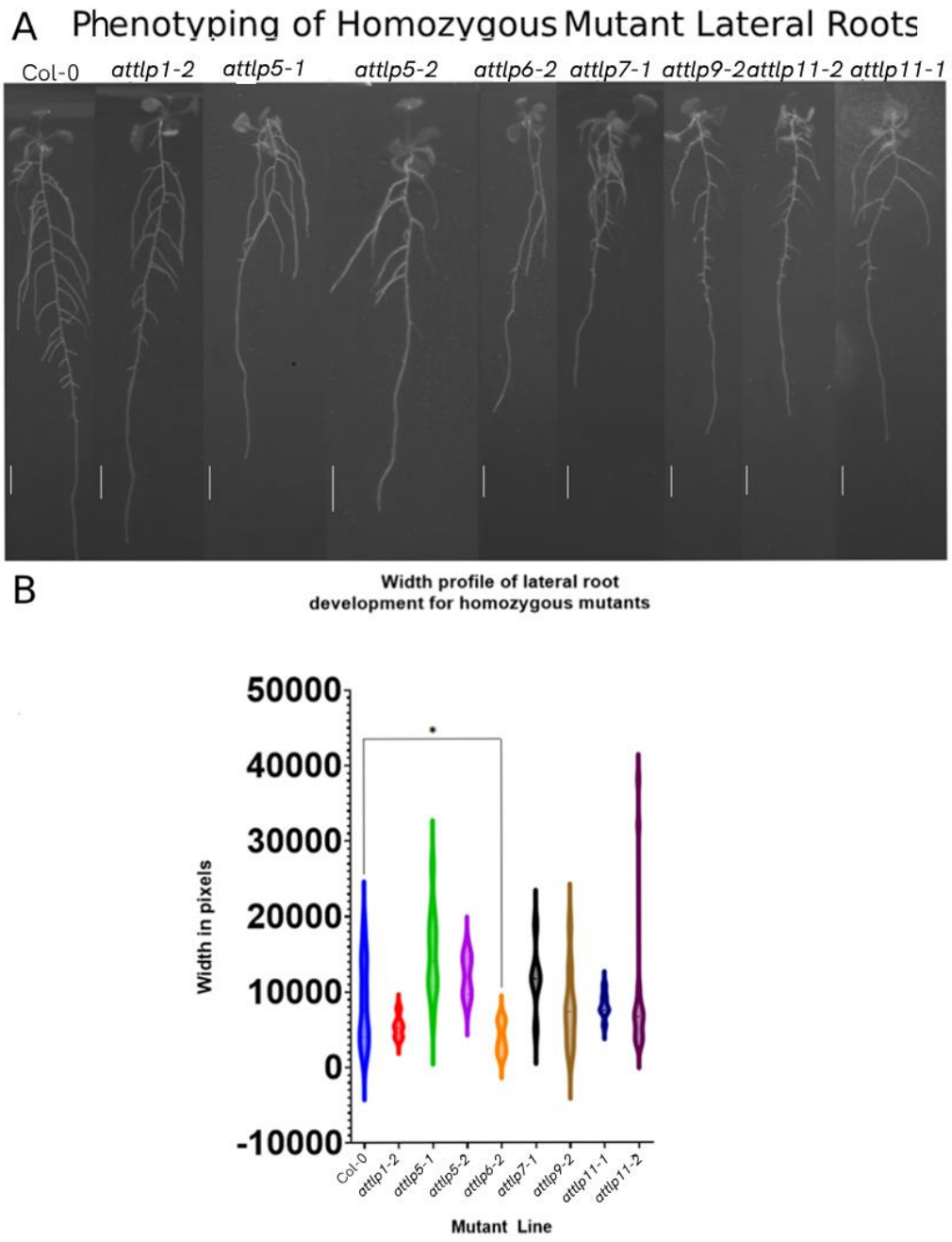

Figure 8 A. Single individuals from each successfully genotyped line, these photos were analysed for lateral root structure analysis through RootNav. B. Representative samples for each Mutant type that was considered as sucturally similar to HvEGT1. White bars represent 5mm for each sample.

B. A violin plot showing the width profile of *attlp* mutants that showed significant difference in primary root bending. Mutant *attlp6-2* showed a significantly narrower profile than Col-0 (n=14), with the steeper lateral structure of *attlp6-2* showing a p value of p= 0.0201 n=5 with a Welch's T-test. This is annotated with the line and asterisk.

Expression of AtTLPs in root tissues

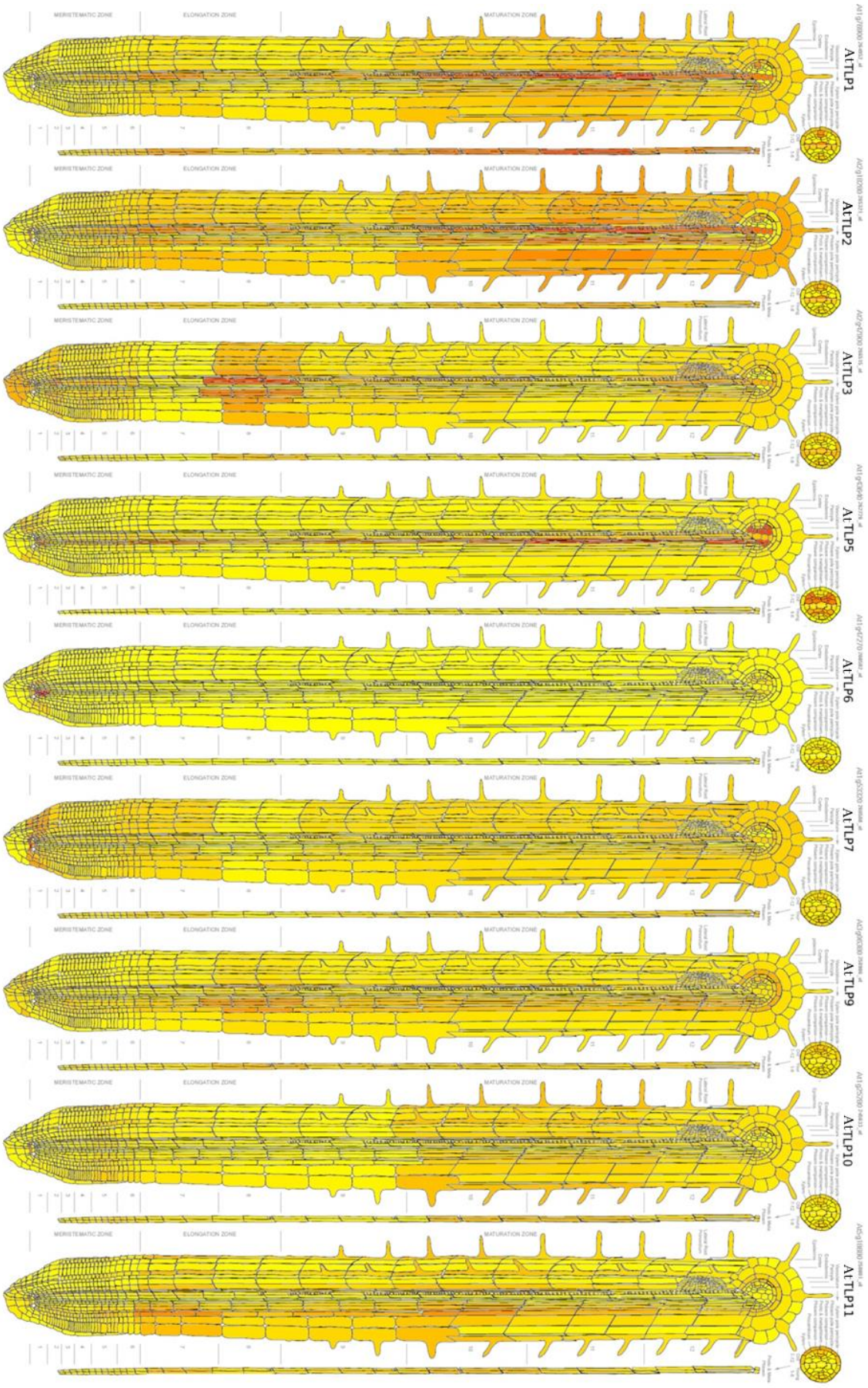

Figure 9. Tissue specific expression of AtTLPs as generated with the Tissue Specific Root from the ePlant database [31]. The image shows high expression in red and low in yellow.

The tissue specific expression of the AtTLPs showed a high level of expression within the elongation zone for AtTLPs 1,2,3,9, and 11. However, AtTLPs 1, 2 and 5 all show high levels of expression within the maturation zone. AtTLP6 shows the highest level of expression within the meristematic zone, specifically in the quiescent centre. The expression of all AtTLPs within the root provides further indication that the gene family may have a function within the root tissue.

Discussion

The study of AtTLPs reveals intriguing trends in subcellular localization, phylogeny, and functional redundancy, particularly concerning their role in root angle regulation. Notably, HvEGT1 shows a strong peroxisomal localization, supporting its involvement in hydrogen peroxide catabolism, which may explain the enhanced gravitropic bending in *hvegt1* mutants [8]. Despite some mixed results, trends across attlp mutants, including *attlp2, attlp3, attlp6, attlp9,* and *attlp11*, suggest complex regulatory mechanisms, with *attlp6* displaying a unique and more pronounced bending response. Interestingly, while *attlp6* mutants showed a faster bending rate, this was coupled with significantly reduced growth rates and poor seed viability, complicating interpretations. The limited seed viability raises questions about selection bias and the reliability of the observed phenotype. If the poor germination was unrelated to AtTLP6 silencing, it could indicate the involvement of other factors. The study's limited scope, due to time constraints, restricted the ability to fully explore these aspects, warranting larger-scale investigations to obtain statistically robust data.

The functional redundancy between certain AtTLPs is evident, particularly when considering the double mutant *attlp2-2 attlp3-1*, which exhibited a narrower lateral root system, contrasting with the lack of significant bending in the single mutants. This supports the idea of overlapping biochemical functions. Previous studies have highlighted the plasma membrane localization of AtTLPs 3 and 9, their roles in abscisic acid (ABA) and osmotic stress responses, and their functional redundancy [13], further reinforcing the concept of biochemical redundancy among AtTLPs in stress signalling pathways. To test the hypothesis of redundancy, seeds from higher-order mutants (e.g., *attlp2 attlp6* and *attlp2 attlp10*) were analysed, showing no significant growth differences compared to controls, except for *attlp2 attlp6 attlp10* which failed to grow, echoing the poor viability observed in *attlp6* within our own experiment. This raises the possibility that the TLP6 growth defect in our experiments was either due to poor seed quality or a non-homozygous mutation. Further genotyping and experimentation are needed to draw definitive conclusions, with an emphasis on the importance of performing a qRT-PCR on the mutant lines to quantify the gene expression levels. This is as without that data the study cannot definitively demonstrate the extent to which the expression of the AtTLPs were lowered or silenced in the mutants tested. This is especially important as many of the T-DNA inserts are not exonic, which lowers the chances of the T-DNA accurately silencing the expression of the functional protein.

The localization of AtTLPs in various subcellular compartments, including the plastid for AtTLP6, points to a potential role in reactive oxygen species (ROS) management. The apoplast, mitochondria, and plastids are key sites for H_2O_2 production, a central component in ROS signalling [32]. This aligns with the predicted localization of AtTLP6 and its involvement in plastid-related functions. AtTLP3, in particular, is involved in stress-induced signalling, being downregulated upon H_2O_2 treatment, further implicating AtTLPs in ROS-mediated responses [32]. One potential explanation for the lack of significant bending in AtTLP2 mutants, despite its similarity to HvEGT1, lies in its inability to interact with ASK proteins, a key component of SCF-type E3 ligase complexes. In contrast, AtTLP6 uniquely interacts with ASK1, ASK2, and ASK11, while other AtTLPs primarily interact with ASK1 [33]. The delayed growth and high seedling mortality observed in *attlp6* mutants

could be linked to these interactions, as *ask1* and *ask2* mutants show severe growth defects. The proposed higher-order mutant of *attlp2, attlp3, attlp9,* and *attlp11* would help elucidate whether ASK1 and ASK2 interactions drive the AtTLP-mediated phenotypes observed. However, this could also be due to the AtTLP6 being involved in pollen development, where mutant plants produced 15% of pollen with misarranged male germ units and 5–10% aborted grains [34]. The overexpression of AtTLP6 was also shown to result in severely dwarfed plants [35], indicating that altered levels of AtTLP6 can have significant developmental consequences that may extend to seed development and viability.

In figure 8, AtTLP6 showing expression in the root tip meristem suggests potential roles in actively growing regions of the Arabidopsis root, although not specifically in the stele and cortex of the basal meristem and transition zone like HvEGT1. However, the root tip is the primary sensory organ of the root, detecting various environmental cues [36] and as previous studies mention, the gravitropic mechanisms has been observed within the tip of the root in Arabidopsis [8]. If AtTLP6 were expressed here, it could play a role in mediating responses to these cues, potentially involving ROS signalling in as was noted in other studies for AtTLP3 and AtTLP9 [13]. This is as within the root tip is the quiescent centre, which is crucial for maintaining the balance between cell division and differentiation in the surrounding stem cells [37]. If AtTLP6, as an F-box protein, is expressed in the quiescent centre it could support the idea that it would be involved in targeting specific proteins for degradation via SCF E3 ligase complexes. Notably, *ask1 ask2* double mutants exhibit defects in cell division in the root tips [38] , highlighting the importance of ASK proteins, with which AtTLP6 and other AtTLPs interacts with in this region. HvEGT1 in barley is highly expressed in the stele and cortical tissues within the basal meristem and transition zone of the root, with its expression then decreases and becomes undetectable in the maturation zone [8] . This specific localisation indicates a role in these inner root tissues during elongation, therefore influencing root angle via an auxin independent AGO mechanism. The AtTLP that matches this expression pattern the most is AtTLP3, further indicating that, while not supplying a significant difference in bending within the single mutant, a similar function may be present as demonstrated by the further bending in the *attlp2 attlp3* double mutant than control. This could also suggest that, while showing a similar result in controlling root bending, AtTLP6 may not be following a similar mechanism of root bending control.

Additionally, the complexity of ROS regulation in relation to AtTLP function suggests that further research, including quantitative PCR and transcriptome analysis, is needed to confirm expression levels in the mutants. A transgenic rescue experiment, introducing HvEGT1 into the AtTLP6 mutant background, would be particularly valuable in establishing an orthologous relationship between these proteins and confirming their roles in root angle regulation [39].

In conclusion, while the data presented provide intriguing insights into the roles of AtTLPs in root angle regulation, stress signalling, and ROS management, the limitations of the study call for further investigations. Future experiments, such as generating higher-order mutants and examining AtTLP-ASK interactions, will be crucial in fully understanding the mechanistic roles of AtTLPs in root regulation. .

Conclusion

This study demonstrates the importance of understanding the mechanisms that impact root architecture, which is crucial for the adaption of crops due to changing environmental conditions. Here we have shown a possible relationship between AtTLP6 and HvEGT1, which may suggest a conserved function of similar AtTLPs on root bending outside of the cereal specific homologs previously observed. While our research did show promising trends in the increasing of bending speeds in many AtTLPs such as AtTLPs 2,3,6,9, and 11, further investigations are necessary to confirm the involvement of AtTLPs aside from AtTLP6 in gravitropic and anti-gravitropic offset mechanisms.

The mixed results of our experiments, in particular the impacts of AtTLP6 in both root bending and growth, highlight the complexity of AtTLP functions and suggest that this is an area of study that requires more attention, as it has not been properly covered in previous research. The discrepancies in seed viability, as well as the lack of consistency due to the complex systems that regulate root angle indicate that further transcript analysis and the phenotyping of higher-order mutants is required before we can feel secure in our findings. Further work should also focus on the interaction of AtTLPs with ASK proteins, especially the unique interactions between ASK2 and AtTLP6, which may go towards explaining the observed differences in root bending compared to other AtTLPs.

The wider implications of this study go beyond Arabidopsis, as demonstrating a conserved function for TLPs in root architecture across plant species could contribute to the development of crops better equipped to handle abiotic stresses such as drought and increasing salinity. The knocking out of HvEGT1 and AtTLP6 can act as a gene-editable means to achieve a steep root angle, which would likely provide crop varieties with increased nitrogen-capture and drought tolerance traits. Furthermore, the identification of AtTLP6 as a homolog for HvEGT1 could form a foundation for using this model organism to expedite researching, if the issues of seed viability can be overcome, this could lead to the more rapid and efficient analysis of the mechanisms of root angle control. Ultimately, the findings of this study underscore the potential of manipulating the expression of TLPs to optimize root architecture in a given environment, which is critical for future agricultural resilience in the face of climate change.

Acknowledgement

I would like to acknowledge the Dept of Plant Sciences and School of Biosciences at Nottingham for providing the funding for this MRes project linked to BBSRC funded project focusing on understanding how EGT1 controls root angle in crops. I would also like to thank Rahul Bhosale, Adam Binns, Atish Bansod, and all the other members of the plant science team for the opportunity and help throughout my project.

References

1. Monshausen, G.B., , and S. Gilroy, *The exploring root — root growth responses to local environmental conditions.* Current Opinion in Plant Biology, 2009/12/01. **12**(6).
2. Lynch, J.P., *Root phenotypes for improved nutrient capture: an underexploited opportunity for global agriculture*. New Phytologist, 2019/07/01. **223**(2).
3. Mukherjee, S., et al., *Climate Change and Drought: a Perspective on Drought Indices*. Current Climate Change Reports 2018 4:2, 2018-04-23. **4**(2).
4. Ditengou, F.A., W.D. Teale, and K. Palme, *Settling for Less: Do Statoliths Modulate Gravity Perception?* Plants, 2020/01. **9**(1).
5. Dieter Volkmann, F.B., Irene Lichtscheidl, Dominique Driss-Ecole, Gérald Perbal, *Statoliths motions in gravity-perceiving plant cells: does actomyosin counteract gravity?* The FASEB Journal, 1999. **13**(9001).
6. Kawamoto, N. and M.T. Morita, *Gravity sensing and responses in the coordination of the shoot gravitropic setpoint angle*. New Phytologist, 2022/12/01. **236**(5).
7. DIGBY, J. and R.D. FIRN, *The gravitropic set-point angle (GSA): the identification of an important developmentally controlled variable governing plant architecture**. Plant, Cell & Environment, 1995/12/01. **18**(12).
8. Fusi, R., et al., *Root angle is controlled by EGT1 in cereal crops employing an antigravitropic mechanism*. Proceedings of the National Academy of Sciences, 2022-7-26. **119**(31).
9. Roychoudhry, S., et al., *The developmental and environmental regulation of gravitropic setpoint angle in Arabidopsis and bean*. Scientific Reports 2017 7:1, 2017-03-03. **7**(1).

10. Smith, S. and I.D. Smet, *Root system architecture: insights from Arabidopsis and cereal crops*. Philosophical Transactions of the Royal Society B: Biological Sciences, 2012-6-5. **367**(1595).
11. *Modeling Crop Root Growth and Function*. Advances in Agronomy Volume 44, 1990/01/01. **44**.
12. G.K.K., et al., *Genetic regulation of the root angle in cereals*. Trends in Plant Science, 2024/07/01. **29**(7).
13. Bao, Y., et al., *Characterization of Arabidopsis Tubby-like proteins and redundant function of AtTLP3 and AtTLP9 in plant response to ABA and osmotic stress*. Plant Molecular Biology 2014 86:4, 2014-08-29. **86**(4).
14. Koornneef, M. and D. Meinke, *The development of Arabidopsis as a model plant*. The Plant Journal, 2010/03/01. **61**(6).
15. Zhao, D., et al., *Members of the Arabidopsis-SKP1-like Gene Family Exhibit a Variety of Expression Patterns and May Play Diverse Roles in Arabidopsis*. Plant Physiology, 2003/09. **133**(1).
16. Scholl, R.L., S.T. May, and D.H. Ware, *Seed and Molecular Resources for Arabidopsis*. Plant Physiology, 2000/12/01. **124**(4).
17. *Insertional mutagenesis of genes required for seed development in Arabidopsis thaliana - PubMed*. Genetics, 2001 Dec. **159**(4).
18. *Genome-wide insertional mutagenesis of Arabidopsis thaliana - PubMed*. Science (New York, N.Y.), 08/01/2003. **301**(5633).
19. Fink, F., *Extraction of genomic DNA using*. 2016.
20. Holm, L., et al., *Searching protein structure databases with DaliLite v.3*. Bioinformatics, 2008/12/12. **24**(23).
21. Mutte, S.K. and D. Weijers, *High-resolution and deep phylogenetic reconstruction of ancestral states from large transcriptomic data sets*. Bio-protocol, 2020. **10**(6): p. e3566-e3566.
22. Mukhopadhyay, S., et al., *The tubby family proteins*. Genome Biology 2011 12:6, 2011-06-28. **12**(6).
23. Holm, L., et al., *DALI shines a light on remote homologs: One hundred discoveries*. Protein Science, 2023/01/01. **32**(1).
24. Lai, C.-P., et al., *Molecular Analyses of the Arabidopsis TUBBY-Like Protein Gene Family*. Plant Physiology, 2004/04/01. **134**(4).
25. Whisstock, J.C. and A.M. Lesk, *Prediction of protein function from protein sequence and structure | Quarterly Reviews of Biophysics | Cambridge Core*. Quarterly Reviews of Biophysics, 2003/08. **36**(3).
26. Sahu, S.S., C.D. Loaiza, and R. Kaundal, *Plant-mSubP: a computational framework for the prediction of single- and multi-target protein subcellular localization using integrated machine-learning approaches*. AoB PLANTS, 2020/05/01. **12**(3).
27. Saitou, N. and M. Nei, *The neighbor-joining method: a new method for reconstructing phylogenetic trees*. Molecular Biology and Evolution, 1987/07/01. **4**(4).
28. *Confidence Limits on Phylogenies: An Approach Using the Bootstrap*. Evolution, 1985. **39**(4).
29. *Evolutionary Divergence and Convergence in Proteins*. Evolving Genes and Proteins, 1965/01/01.
30. Tamura, K., G. Stecher, and S. Kumar, *MEGA11: Molecular Evolutionary Genetics Analysis Version 11*. Molecular Biology and Evolution, 2021/06/25. **38**(7).
31. Waese, *Tissue specific Root*. 2017.
32. Reitz, M.U., et al., *The Subcellular Localization of Tubby-Like Proteins and Participation in Stress Signaling and Root Colonization by the Mutualist Piriformospora indica*. Plant Physiology, 2012/09/03. **160**(1).
33. Chia-Ping, L. and S. Jei-Fu, *Interaction analyses of Arabidopsis tubby-like proteins with ASK proteins*. Botanical studies, 2012. **53**(4).
34. Reňák, D., et al., *Wide-scale screening of T-DNA lines for transcription factor genes affecting male gametophyte development in Arabidopsis*. Sexual Plant Reproduction 2011 25:1, 2011-11-20. **25**(1).
35. Devendrakumar, K.T., et al., *Arabidopsis Tubby domain-containing F-box proteins positively regulate immunity by modulating PI4Kβ protein levels*. New Phytologist, 2023/10/01. **240**(1).

36. Bano, N., et al., *Tubby-like proteins (TLPs) transcription factor in different regulatory mechanism in plants: a review.* Plant Molecular Biology 2022 110:6, 2022-10-18. **110**(6).
37. Strotmann, V.I. and Y. Stahl, *At the root of quiescence: function and regulation of the quiescent center.* Journal of Experimental Botany, 2021/10/13. **72**(19).
38. Liu, F., et al., *The ASK1 and ASK2 Genes Are Essential for Arabidopsis Early Development.* The Plant Cell, 2004/01/02. **16**(1).
39. Ecovoiu, A.A., et al., *Inter-Species Rescue of Mutant Phenotype—The Standard for Genetic Analysis of Human Genetic Disorders in Drosophila melanogaster Model.* International Journal of Molecular Sciences, 2022/03. **23**(5).